System Identification from Output Measurements

Rytter, Anders; Jensen, Jacob Laigaard; Hansen, Lars Pilegaard

Publication date:
1989

Document Version
Early version, also known as pre-print

INSTITUTTET FOR BYGNINGSTEKNIK

INSTITUTE OF BUILDING TECHNOLOGY AND STRUCTURAL ENGINEERING

AALBORG UNIVERSITETSCENTER · AUC · AALBORG · DANMARK

FRACTURE AND DYNAMICS
PAPER NO. 15

Paper to be presented at the Eighth International Modal Analysis Conference, January 29 - February 1, 1990, Orlando, Florida, USA, sponsored by Society for Experimental Mechanics,Inc. and Union College

A. RYTTER, J. LAIGAARD JENSEN & L. PILEGAARD HANSEN

SYSTEM IDENTIFICATION FROM OUTPUT MEASUREMENTS

NOVEMBER 1989 ISSN 0902-7513 R8929

INSTITUTTET FOR BYGNINGSTEKNIK

INSTITUTE OF BUILDING TECHNOLOGY AND STRUCTURAL ENGINEERING

AALBORG UNIVERSITETSCENTER · AUC · AALBORG · DANMARK

FRACTURE AND DYNAMICS
PAPER NO. 15

Paper to be presented at the Eighth International Modal Analysis Conference, January 29 - February 1, 1990, Orlando, Florida, USA, sponsored by Society for Experimental Mechanics,Inc. and Union College

A. RYTTER, J. LAIGAARD JENSEN & L. PILEGAARD HANSEN

SYSTEM IDENTIFICATION FROM OUTPUT MEASUREMENTS

NOVEMBER 1989 ISSN 0902-7513 R8929

SYSTEM IDENTIFICATION FROM OUTPUT MEASUREMENTS

Anders Rytter
Rambøll & Hannemann A/S
Kjærulfsgade 2, DK-9400 Nørresundby

Jakob Laigaard Jensen & L. Pilegaard Hansen
Institute of Building Technology and Structural Engineering
University of Aalborg
Sohngaardsholmsvej 57, DK-9000 Aalborg

ABSTRACT

The basic assumption in the classical system identification methods is that reliable information about both the system inputs and the system outputs can be obtained by measurements on the structure. However dealing with the system identification of a dynamic excited offshore structure this method is not direct applicable, because the environmental loads can not be estimated with the required accuracy.

Therefore there is a need for system identification methods which provide reliable estimates of the dynamic characteristica of a structure when only the system output due to a natural dynamic and random environmental load is known.

The purpose of this paper is to present and compare three more or less advanced system identification methods, which are based upon output measurements and applicable for system identification of lightly damped structures. The comparison of the three methods will be based upon simulated and experimental output data for a model of a monopile structure.

NOMENCLATURE

ω_i : The ith cyclic eigen frequency (rad/sec)

ω : Cyclic frequency (rad/sec)

j, k : index

i : $\sqrt{-1}$,index

B_e : Resolution bandwidth (rad/sec)

B_i : Half power bandwidth (rad/sec)

$*$: Complex conjugate

N : Number of degree of freedom

$\Delta\omega$: Frequency range (rad/sec)

N_S : Number of points in spectra

N_R : Number of measuring points

K_k, K_i, K_W : Constant

m_i : Mass at node i

ζ_i : The ith modal damping ratio

$\tilde{\phi}_{ik}$: Element of the weighted modal matrix

T : Upper index. Theoretical

M : Upper index. Measured

F : Errorfunction

A : Constant

$G_{F_iF_i}(\omega)$: Auto spectrum of the excitation

$G_{X_BX_B}(\omega)$: Auto spectrum for base acceleration

$G_{\ddot{X}_i\ddot{X}_j}(\omega)$: Cross spectrum of accelerations

$\Theta_{\ddot{X}_i\ddot{X}_j}(\omega)$: Phase angel spectrum for accelerations

$G_{noise}(\omega)$: White noise process

$H_k(\omega)$: Frequency response function of the kth mode

1 INTRODUCTION

The performance of dynamic field measurements on offshore structures and thereby the use of system identification methods has been increased extensively during the last decade. The purpose of the field measurements has been to verify and update the analytical design model and/or to detect damages in the structure.

The basic assumption in the classical system identification method is that reliable information about both the system inputs (e.g. forces) and the system outputs (e.g. accelerations) can be obtained by measurements on the structure. However dealing with the system identification of a dynamic excited offshore structure this method is not direct applicable, because the forces due to the environmental loads cannot be estimated with the required accuracy. The forces must instead be determined by means of theoretical models, which

are based upon a few measured/observed parameters of the environmental loads such as the significant wave height and zero upcrossing period. Therefore there is a need for system identification methods which provide reliable estimates of the dynamic characteristica (eigen frequencies, damping ratios) of a structure when only the system output is known.

The purpose of this paper is to present and compare three different system identification methods based upon output measurements. The comparison of the three methods will be based upon simulated and experimental output data for a 4 m high model of a monopile structure. The monopile platform has been considered as a two degree of freedom system during the tests based upon simulation. The model and the test equipment has been described in detail in an earlier report made by Jensen (see Jensen [2]).

2 GENERAL MODEL

The cross spectrum of the accelerations $G_{\ddot{X}_i\ddot{X}_j}(\omega)$ of the two masses in the 2 DOF system shown in figure 1 is given by (1), when the structure is subjected to a random excitation at the base , and by (2) when the structure is subjected to a random excitation at the 2 masses .

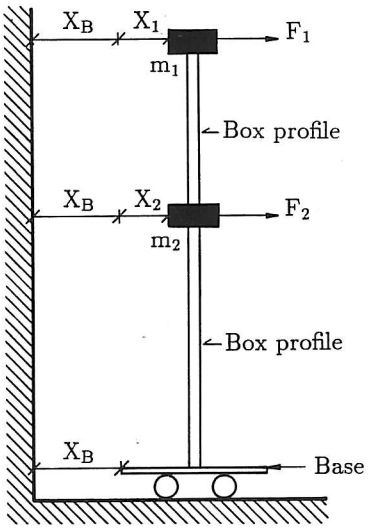

Figure 1. 2 DOF system.

$$G_{\ddot{X}_i\ddot{X}_j}(\omega) = \omega^4 \sum_{k=1}^{N}\sum_{l=1}^{N} \tilde{\phi}_{ik}\tilde{\phi}_{jl}H_k^*(\omega)H_l(\omega) \sum_{i_1=1}^{N} \tilde{\phi}_{i_1k}m_{i_1} \sum_{i_2=1}^{N} \tilde{\phi}_{i_2k}m_{i_2}G_{\ddot{X}_B\ddot{X}_B}(\omega) \quad (1)$$

$$G_{\ddot{X}_i\ddot{X}_j}(\omega) = \omega^4 \sum_{k=1}^{N}\sum_{l=1}^{N} \tilde{\phi}_{ik}\tilde{\phi}_{jl}H_k^*(\omega)H_l(\omega) \sum_{i_1=1}^{N}\sum_{i_2=1}^{N} \phi_{ki_1}\phi_{li_2}G_{F_lF_k}(\omega). \quad (2)$$

$$H_k(\omega) = \frac{1}{\omega_k^2 - \omega^2 + 2\omega_k\omega\zeta_k i} \quad (3)$$

The analysis presented in this paper includes the use of the two force spectra shown in (4) and (5).

$$\text{Spectrum no. } 1: \quad G_{F_2F_2}(\omega) = A \quad (4)$$

$$\text{Spectrum no. } 2: \quad G_{\ddot{X}_B\ddot{X}_B}(\omega) = A\omega^4 \quad (5)$$

The first spectrum correspond to the situation, where the system is excited with a white noise process at the mass no. 2,see figure no. 1.

The second spectrum correspond to the situation, where the system is excited with a white noise displacement process at the base.

Realizations of the two spectra has been simulated by summation of a sufficient large numbers of cosines.

The system output (i.e. the acceleration processes for the two masses) has been calculated by means of the computer program PROGSIM, which has been developed in connection with the present simulation tests. PROGSIM performs a numerical integration of the equations of motion by means of the Runge- Kutta algoritme (see e.g. Thomson [3]). The integration is based upon start conditions, load processes, mass- , damping- and stiffness matrices specified by the user.

3 PRESENTATION OF THE METHODS

This chapter describes the basic ideas in the three identification methods and gives some rules of thumb for the limits for the application of the methods.

3.1 The Simple Method.

The first identification method to be described is very simple and due to this fact called "The Simple Method" (hereafter denoted SM). In spite of the simplicity the method gives good rough estimates for eigen frequencies, normal mode shapes and damping ratios in many cases where only the system output is known. The method or part of it has because of the simplicity been used by many investigators .

The method is only applicable, when the conditions given below are fulfilled. The boundaries given in the conditions are taken from Bendat & Piersol [1] .

- Linear system
- Lightly damped system
- Completely decoupled modes
- The analysis resolution bandwidth B_e must be approximately 20 % of the half power point bandwidth B_i of the mode.
- Reasonably uniformed autospectrum of the excitation around the eigen frequencies of the structure (e. g. $G_{F_iF_i}(\omega) \approx$ constant for $\omega_i - 3B_i \leq \omega \leq \omega_i + 3B_i$)

The eigen frequencies of the structure can be identified by means of the autospectra of and the cross spectra between the measuring points. Due to the assumption that the structure is lightly damped and has completely decoupled modes then the autospectrum of the displacements will reach a local maximum at frequencies where either the excitation spectrum peaks or the frequency response function of the structure peaks. The points on the structure will be either in phase or 180° out of phase at frequencies, where the autospectrum of the displacements peaks due to resonance in the structure . Normally the phase between points on the structure will be something other then 0° or 180° at frequencies, where the autospectrum of the displacements peaks due to a spectral peak in the excitation spectrum.

The normal mode shapes are estimated by means of the autospectra (i=j in equation (1) and (2)) for the acceleration. By setting $\omega = \omega_k$ and taken into account that the structure is assumed to be lightly damped, then it will be seen that a approximated value of ϕ_{ik} can be determined by means of (6).

$$\phi_{ik} \approx K_k \sqrt{G_{X_iX_i}(\omega_k)} \tag{6}$$

Errors due to extraneous noise and/or coupling among the modes can be revealed by means of the coherence functions and the phase spectra between all the measurement points. Bendat & Piersol [1] suggest that the autospectrum at specific location should not be used to determine a normal mode shape unless the measurement produces near unity coherence (≥ 0.9) and a phase near to 0° or 180° with all other output measurements.

The modal damping ratios can be estimated by means of the half-power point bandwidth in the auto- and/or cross spectra as given in (7).

$$\zeta_i = \frac{B_i}{2\omega_i} \tag{7}$$

3.2 Local curve fit on response spectra peaks.

The method to be described in this section is called "Local curve fit on response spectra peaks" (hereafter denoted LCF), and it consist of a least square fit of the theoretically frequency response function to an approximately measured frequency response function in the area around the eigen frequencies.

The method is based upon the same assumptions about the system and the autospectrum of the excitation given in section 3.1 for the simple method.

The square of the frequency response function can under these assumptions approximately be expressed by (8) in the frequency domain around the response spectra peaks. Equation (8) has been derived from (1) by omitting terms which only gives small contributes to $G_{\ddot{X}_j X_j}(\omega)$ in the considered frequency domain.

$$|H_i(\omega)|^2 \approx \omega^{-4} \phi_{ji}^{-2} K_W G_{\ddot{X}_j \ddot{X}_j}(\omega) \quad \text{for} \quad \omega_i - \Delta\omega \leq \omega \leq \omega_i + \Delta\omega \tag{8}$$

$\Delta\omega$ is half of the frequency range under consideration. $\Delta\omega$ has been set to $3B_i$ in the analysis presented in this paper.

The square of the frequency response function of the ith eigen mode can in general be written as shown in (9).

$$|H_i(\omega)|^2 = \frac{K_i}{(\omega_i^2 - \omega^2)^2 + (2\omega_i\zeta_i\omega)^2} \tag{9}$$

The system parameters can thus be estimated by fitting the theoretical frequency response function given in (9) to the measured (approximated) frequency response function given by (8) over the considered frequency range. A fitting based upon a minimization of the errorfunction in (10) with respect to ω_i, ζ_i and ϕ_{ji} gives the expressions shown in (11) and (12) for estimates of eigen frequencies, modal damping ratios and relative mode shapes.

$$F = \sum_{k=1}^{N_S} ({}^T|H_i(\omega_k)|^2 - {}^M|H_i(\omega_k)|^2)^2 \tag{10}$$

$$\omega_i = \frac{1}{N_S} \sum_{j=1}^{N_S} \sqrt[4]{\frac{K_C^j}{K_A^j}} \tag{11}$$

$$\zeta_i = \frac{1}{N_S} \sum_{j=1}^{N_S} \sqrt{\frac{1}{2} + \frac{K_B^j}{4\omega_i^2 K_A^j}} \quad , \quad |\frac{\phi_{lk}}{\phi_{jk}}| = \sqrt{\frac{K_A^j}{K_A^l}} \tag{12}$$

where K_A^j, K_B^j and K_C^j are given by equation (13)-(18).

$$K_A^j = \frac{c_2^j a_1 - c_1^j a_3}{a_2 a_1 - a_3^2} \quad , \quad K_B^j = \frac{c_2^j a_3 - c_1^j a_2}{a_2 a_1 - a_3^2} \tag{13}$$

$$K_C^j = \frac{1}{N_S}(\sum_{i=1}^{N_S} S_i^j - K_A^j \sum_{i=1}^{N_S} \omega_i^4 - K_B^j \sum_{i=1}^{NS} \omega_i^2) \tag{14}$$

$$a_k = N_S \sum_{i=1}^{N_S} \omega_i^{4k} - (\sum_{i=1}^{N_S} \omega_i^{2k})^2 \quad \text{for} \quad k = 1,2 \tag{15}$$

$$a_3 = N_S \sum_{i=1}^{N_S} \omega_i^6 - (\sum_{i=1}^{N_S} \omega_i^4)(\sum_{i=1}^{N_S} \omega_i^2) \quad (16)$$

$$c_k^j = N_S \sum_{i=1}^{N_S} (S_i^j \omega_i^{2k}) - \sum_{i=1}^{N_S} S_i^j \sum_{i=1}^{N_S} \omega_i^{2k} \quad \text{for} \quad k = 1,2 \quad (17)$$

$$S_i^j = \frac{\omega_i^4}{G_{\ddot{X}_j \ddot{X}_j}(\omega_i)} \quad (18)$$

The sign of the ratio $|\frac{\phi_{lk}}{\phi_{jk}}|$ given in (12) has to be determined by means of the phase angel $\Theta_{\ddot{X}_l \ddot{X}_j}(\omega_k)$.

3.3 Global curve fit on response spectra.

The last identification method to be described is a curve fitting method in the frequency domain, which gives estimates of the input spectrum and for the dynamic characteristica of the system. The method is hereafter denoted GCF . The estimates for the input spectrum will be given as parametric model. The dynamic characteristica of the system will be expressed by means of normal mode shape vectors, modal damping ratios and eigen frequencies.

The basic idea in the method is to minimize the errorfunction F given in (19).

$$F = \sum_{i=1}^{N_R} \sum_{k=1}^{N_S} (G_{X_i X_i}^T(\omega_k) - G_{X_i X_i}^M(\omega_k))^2 \quad (19)$$

where $G_{X_i X_i}^T(\omega_k)$ is the theoretical spectrum (see i.e. equation (1) and (2)) and $G_{X_i X_i}^M(\omega_k)$ is the measured spectrum.

The minimization of F is in this paper performed by means of the computer program NLPQL [4]. Dealing with more complicated structures it could be useful to set up some additionally constraints based upon ordinary physically requests and a priori knowledge about the structure.

4 TEST OF THE METHODS

The three methods have been tested for four situations with simulated data and one with experimental data, see table no. 1.

Test no.	Test type	Load type
1	Simulation	White noise load proc. at mass 2
2	Simulation	White noise load proc. at mass 2 + noise
3	Simulation	White noise displacement proc. at base
4	Simulation	White noise displacement proc. at base + noise
5	Model test	White noise displacement proc. at base

Table 1

The output signal from test no. 1 and 3 has been overlayered by a white noise process $G_{noise}(\omega)$ in test no. 2 and 4. $G_{noise}(\omega)$ is given by (20).

$$G_{noise}(\omega) = 0.05 \quad G_{X_1 X_1}(\omega = \omega_1) \quad (20)$$

The system parameters used in the simulation tests are denoted "exact" in the following results.

The FFT-algoritme has been applied to calculate the system outputspectra in the identification methods presented in section 3.1, 3.2 and 3.3. Each sample in the FFT-analysis consisted of 4096 points, which were sampled by a frequency of 50 Hz. The number of averages was 8 in all cases.

Table 2 and 3 shows the estimated and the exact values of the first and second eigen frequency respectively. The results shows that the three methods are equal with respect to determine eigen frequencies. The error is less than 1 % in all cases, which is acceptable. A part of the error is due to the resolution in the performed FFT-analysis.

Method	Test no. 1	Test no. 2	Test no. 3	Test no. 4	Test no. 5
SM	6.98	6.98	6.98	6.98	6.98
LCF	6.98	6.96	6.98	6.96	6.97
GCF	6.98	6.95	6.99	6.95	6.95
Exact	6.98	6.98	6.98	6.98	X

Table 2. First eigen frequency (rad/sec).

Method	Test no. 1	Test no. 2	Test no. 3	Test no. 4	Test no. 5
SM	45.18	45.18	45.18	45.18	45.48
LCF	45.18	45.11	45.18	45.18	45.46
GCF	45.19	45.17	45.18	45.21	45.24
Exact	45.17	45.17	45.17	45.17	X

Table 3. Second eigen frequency (rad/sec).

The estimates for the modal damping ratios are shown in table 4 and 5. From the results it can be seen that the simple method (SM) in all cases leads to an overestimation around 500 %. The overestimation is due to the resolution in FFT- analysis has been to large and the structure is lightly damped. The method based upon local curve fitting on response spectra peaks overestimated the modal damping ratio by around 25 to 3000 % depending on how much noise there is on the output signal. The method gives good estimates for the upper limit of the damping in almost all situations with noiseless output signals. The GCF-method gives the best estimates for the modal damping ratios. The errors are around 5-40 % on the estimates for ζ_1 and less than 6 % on the estimates for ζ_2. The sensitivity of the method against noise is very low. Noise on the output signal seems to lead to under estimation of the modal damping ratios. A better resolution in the FFT-analysis would for all three methods have lead to better estimates.

Method	Test no. 1	Test no. 2	Test no. 3	Test no. 4	Test no. 5
SM	0.56	0.67	0.56	0.67	0.63
LCF	0.163	4.04	0.41	4.05	2.16
GCF	0.122	0.134	0.145	0.122	0.132
Exact	0.127	0.127	0.127	0.127	X

Table 4. First modal damping ratio (%).

Method	Test no. 1	Test no. 2	Test no. 3	Test no. 4	Test no. 5
SM	0.202	0.288	0.202	0.233	0.109
LCF	0.082	0.217	0.081	0.088	0.208
GCF	0.065	0.063	0.067	0.066	0.072
Exact	0.065	0.065	0.065	0.065	X

Table 5. Second modal damping ratio (%).

Table 6 and 7 show the estimated values of the mode shapes. The SM- and LCF-method gives in general good estimates in the tests where the output signal is free of noise. The estimates from the SM-method will approach to 1.00 if the noise is increased. The LCF-method is apparently very unstable in situations with noise on the output signal. The GCF-method gives reasonable results in all situations.

Method	Test no. 1	Test no. 2	Test no. 3	Test no. 4	Test no. 5
SM	0.381	0.431	0.377	0.427	0.35
LCF	0.384	1.238	0.441	1.243	1.067
GCF	0.381	0.421	0.362	0.450	0.375
Exact	0.380	0.380	0.380	0.380	X

Table 6. First mode shape. $\frac{\phi_{21}}{\phi_{11}}$

Method	Test no. 1	Test no. 2	Test no. 3	Test no. 4	Test no. 5
SM	-0.526	-0.577	-0.511	-0.512	-0.52
LCF	-0.521	-0.853	-0.485	-0.494	-0.511
GCF	-0.585	-0.575	-0.590	-0.576	-0.625
Exact	-0.530	-0.530	-0.530	-0.530	X

Table 7. Second mode shape. $\frac{\phi_{12}}{\phi_{22}}$.

5 CONCLUSION

Three more or less advanced system identification methods based upon output measurements have been presented and tested. The tests have concerned the estimation of the eigen frequencies, modal damping ratios and mode shapes of a model of a monopile structure.

The results of the tests shows that the three methods are equal with respect to estimating the eigen frequencies. In the estimation of modal damping ratios and mode shapes the GCF-method is superior to the two other methods. However the GCF-method is very time-consuming. The runs with NLPQL have taken between 4 and 6 CPU-hours on a Micro-Vax computer. The duration depends especially on the number of variables in the optimization problem and the signal to noise ratio. The number of variables has been 11 in the performes analysis. A low signal to noise ratio demands more iterations before convergence is reached in the optimization and thereby an increased duration of the computerrun. This means that it would not be realistic to use the method in present the form, when one is dealing with the system identification of more complicated structures than the one considered in this paper. Instead it would be a good idea to combine the three methods in the following way.

Step 1. Determine the final estimates for the eigen frequencies by means of the SM-method

Step 2. Determine estimates for the mode shapes by means of the SM-method

Step 3. Determine estimates for the mode shapes and the modal damping ratios by means of the LCF-method

Step 4. Choose bounds and start values for the variables to be used in the GCF-method from the results received in step 2 and 3.

Step 5. Use the GCF-method to calculate the final estimates of the modal damping ratios and the mode shapes.

A reduction of the number of spectra points used in the analysis will of course lead to a saving of computer time. A great deal of the spectra points which are sufficient away from the peaks of resonance could be removed from the analysis without causing any reduction in the quality of the analysis. Further the method might be improved by including a weighting function in (19), which favours the areas around the peaks in the spectra where the signal to noise ratio will be high.

ACKNOWLEDGEMENTS

Financial support from the Danish Council for Scientific and Industrial Research is grateful acknowledged.

6 REFERENCES

[1] Bendat, J.S & A.G. Piersol: *Engineering applications of correlation and spectral analysis.* Wiley 1980.

[2] Jensen, Jakob L. : *Dynamic analysis of a monopile model.* Fracture and Dynamics, paper no. 4. The University of Aalborg, September 1988.

[3] Thomson, W.T.: *Theory of vibration with applications.* Prentice-Hall 1981.

[4] Schittkowski, K.: *NLPQL: A FORTRAN Subroutine Solving Constrained Non-Linear Programming Problems.* Annals of Operations Research, 1986.

FRACTURE AND DYNAMICS PAPERS

PAPER NO. 1: J. D. Sørensen & Rune Brincker: *Simulation of Stochastic Loads for Fatigue Experiments.* ISSN 0902-7513 R8717.

PAPER NO. 2: R. Brincker & J. D. Sørensen: *High-Speed Stochastic Fatigue Testing.* ISSN 0902-7513 R8809.

PAPER NO. 3: J. D. Sørensen: *PSSGP: Program for Simulation of Stationary Gaussian Processes.* ISSN 0902-7513 R8810.

PAPER NO. 4: Jakob Laigaard Jensen: *Dynamic Analysis of a Monopile Model.* ISSN 0902-7513 R8824.

PAPER NO. 5: Rune Brincker & Henrik Dahl: *On the Fictitious Crack Model of Concrete Fracture.* ISSN 0902-7513 R8830.

PAPER NO. 6: Lars Pilegaard Hansen: *Udmattelsesforsøg med St. 50-2, serie 1 - 2 - 3 - 4.* ISSN 0902-7513 R8813.

PAPER NO. 7: Lise Gansted: *Fatigue of Steel: State-of-the-Art Report.* ISSN 0902-7513 R8826.

PAPER NO. 8: P. H. Kirkegaard, I. Enevoldsen, J. D. Sørensen, R. Brincker: *Reliability Analysis of a Mono-Tower Platform.* ISSN 0902-7513 R8839.

PAPER NO. 9: P. H. Kirkegaard, J. D. Sørensen, R. Brincker: *Fatigue Analysis of a Mono-Tower Platform.* ISSN 0902-7513 R8840.

PAPER NO. 10: Jakob Laigaard Jensen: *System Identification1: ARMA Models.* ISSN 0902-7513 R8908.

PAPER NO. 11: Henrik Dahl & Rune Brincker: *Fracture Energy of High-Strength Concrete in Compression.* ISSN 0902-7513 R8919.

PAPER NO. 12: Lise Gansted, Rune Brincker & Lars Pilegaard Hansen: *Numerical Cumulative Damage: The FM-Model.* ISSN 0902-7513 R8920.

PAPER NO. 13: Lise Gansted: *Fatigue of Steel: Deterministic Loading on CT-Specimens.*

PAPER NO. 14: Jakob Laigaard Jensen, Rune Brincker & Anders Rytter: *Identification of Light Damping in Structures.* ISSN 0902-7513 R8928.

PAPER NO. 15: Anders Rytter, Jakob Laigaard Jensen & Lars Pilegaard Hansen: *System Identification from Output Measurements.* ISSN 0902-7513 R8929.

Institute of Building Technology and Structural Engineering
The University of Aalborg, Sohngaardsholmsvej 57, DK 9000 Aalborg
Telephone: 45 98 14 23 33 Telefax: 45 98 14 82 43